Antiviral Research 132 (2016) 141–148

Contents lists available at ScienceDirect

Antiviral Research

journal homepage: www.elsevier.com/locate/antiviral

Single-dose treatment with a humanized neutralizing antibody affords full protection of a human transgenic mouse model from lethal Middle East respiratory syndrome (MERS)-coronavirus infection

Hongjie Qiu [a], Shihui Sun [a], He Xiao [b], Jiannan Feng [b], Yan Guo [a], Wanbo Tai [a, c], Yufei Wang [a, c], Lanying Du [c], Guangyu Zhao [a, **], Yusen Zhou [a, *]

[a] State Key Laboratory of Pathogen and Biosecurity, Beijing Institute of Microbiology and Epidemiology, Beijing, China
[b] Beijing Institute of Basic Medical Sciences, Beijing, China
[c] Lindsley F. Kimball Research Institute, New York Blood Center, New York, NY, USA

ARTICLE INFO

Article history:
Received 30 March 2016
Received in revised form
19 May 2016
Accepted 12 June 2016
Available online 14 June 2016

Keywords:
MERS-CoV
Receptor-binding domain
Humanized monoclonal antibody
Protection
Treatment
Lethal infection

ABSTRACT

Middle East respiratory syndrome coronavirus (MERS-CoV) is continuously spreading and causing severe and fatal acute respiratory disease in humans. Prophylactic and therapeutic strategies are therefore urgently needed to control MERS-CoV infection. Here, we generated a humanized monoclonal antibody (mAb), designated hMS-1, which targeted the MERS-CoV receptor-binding domain (RBD) with high affinity. hMS-1 significantly blocked MERS-CoV RBD binding to its viral receptor, human dipeptidyl peptidase 4 (hDPP4), potently neutralized infection by a prototype MERS-CoV, and effectively cross-neutralized evolved MERS-CoV isolates through recognizing highly conserved RBD epitopes. Notably, single-dose treatment with hMS-1 completely protected hDPP4 transgenic (hDPP4-Tg) mice from lethal infection with MERS-CoV. Taken together, our data suggest that hMS-1 might be developed as an effective immunotherapeutic agent to treat patients infected with MERS-CoV, particularly in emergent cases.

1. Introduction

Middle East respiratory syndrome coronavirus (MERS-CoV), first isolated from a Saudi Arabian patient in September 2012 (Zaki et al., 2012), causes human infection in other parts of the world and thus has become a global concern. In particular, an outbreak in South Korea in 2015 resulted in 186 infections with 36 deaths (http://www.who.int/csr/don/21-july-2015-mers-korea/en/). As of March 16, 2016, a total of 1,690 laboratory-confirmed cases including over 600 deaths have been reported (http://www.who.int/emergencies/mers-cov/en/), representing a mortality rate of 36%. The symptoms caused by MERS-CoV are similar to those from severe acute respiratory syndrome coronavirus (SARS-CoV), a related coronavirus with a 10% fatality rate that led to the 2002–2003 epidemic (Skowronski et al., 2004; Zhong et al., 2003). Unlike SARS-CoV, for which no additional cases have been reported since 2005 (Du et al., 2009), MERS-CoV has shown continually increasing numbers of cases, particularly in Saudi Arabia, suggesting its potential future epidemic status. Nevertheless, no clinically approved vaccines or antiviral therapeutics are currently available, highlighting the urgent need of potent strategies to combat this virus.

MERS-CoV belongs to the *Betacoronavirus* genus of the coronavirus family (de Groot et al., 2013; Zaki et al., 2012). Its spike protein, consisting of S1 and S2 subunits, plays important roles in viral entry into host cells (Bonavia et al., 2003; Gao et al., 2013; Xu et al., 2004). MERS-CoV depends on the receptor-binding domain (RBD) in the S1 subunit to bind to its viral receptor, human dipeptidyl

Abbreviations: CPE, cytopathic effect; EC_{50}, half-maximal effective concentration; hDPP4, human dipeptidyl peptidase 4; MERS-CoV, Middle East respiratory syndrome coronavirus; mAb, monoclonal antibodies; ND_{50}, 50% neutralizing dose; PCR, polymerase chain reaction; RBD, receptor binding domain; SDS-PAGE, sodium dodecyl sulphate-polyacrylamide gel electrophoresis; SPR, surface plasmon resonance; $TCID_{50}$, 50% tissue culture infective dose; V_H, variable region of the heavy chain; V_L, variable region of the light chain.

* Corresponding author. State Key Laboratory of Pathogen and Biosecurity, Beijing Institute of Microbiology and Epidemiology, Beijing, 100071, China.
** Corresponding author. State Key Laboratory of Pathogen and Biosecurity, Beijing Institute of Microbiology and Epidemiology, Beijing, 100071, China.
E-mail addresses: guangyu0525@163.com (G. Zhao), yszhou@bmi.ac.cn (Y. Zhou).

http://dx.doi.org/10.1016/j.antiviral.2016.06.003

peptidase 4 (hDPP4), on the host cell surface, following which the S2 subunit undergoes a dramatic conformational change to allow for membrane fusion and subsequent MERS-CoV penetration into the cellular membrane (Gao et al., 2013; Lu et al., 2013; Raj et al., 2013; Wang et al., 2013). Therefore, the entry of MERS-CoV into target cells might be prevented by either blocking RBD/DPP4 viral receptor binding or by inhibiting MERS-CoV/host cell membrane fusion.

Vaccines and passive therapeutics are effective approaches against viral infections. In general, vaccines cannot provide immediate prophylactic protection against or treatment of ongoing viral infection. In comparison, passive therapeutics based on neutralizing monoclonal antibodies (mAbs) has emerged as a powerful tool to provide prophylactic and therapeutic protection against viral infection (Du et al., 2013a; Zhu et al., 2013). Several human or humanized viral-neutralizing mAbs have been developed, almost all of which target the RBD (Corti et al., 2015; Jiang et al., 2014; Li et al., 2015; Pascal et al., 2015; Tang et al., 2014; Ying et al., 2014; Yu et al., 2015), further suggesting that MERS-CoV RBD represents an ideal target for neutralizing mAb development.

We previously developed a murine mAb, Mersmab1, that targets MERS-CoV RBD and potently neutralizes MERS-CoV infection (Du et al., 2014). Here, we humanized Mersmab1 and generated a humanized mAb, hMS-1, which exhibited high affinity RBD binding. We first investigated the activity as well as the mechanism of hMS-1 in neutralizing MERS-CoV cell entry. Second, we evaluated its ability to neutralize emergent MERS-CoV strains. Finally, we demonstrated that single-dose treatment with hMS-1 was able to elicit full protection against lethal MERS-CoV infection in an hDPP4 transgenic (hDPP4-Tg) mouse model. Of note, hMS-1 represents the first mAb reported to exhibit this capacity to protect treated animals from the lethal infection of MERS-CoV.

2. Materials and methods

2.1. Ethics statement

Animal studies were performed in strict accordance with the recommendations of the Guide for the Care and Use of Laboratory Animals. The animal protocol was approved by the IACUC of the Laboratory Animal Center, State Key Laboratory of Pathogen and Biosecurity, Beijing Institute of Microbiology and Epidemiology (Permit number, BIME 2015-0023). All procedures involving MERS-CoV were carried out in an approved biosafety level 3 facility.

2.2. Preparation of recombinant proteins

MERS-CoV RBD proteins were prepared as previously described (Ma et al., 2014). Briefly, MERS-CoV RBDs (GenBank accession no. AFS88936.1, residues 377–588 of the spike protein) fused with a C-terminal human Fc or His_6 tag were transiently expressed in a 293T cell culture system and purified using HiTrap Protein A FF (Fc-fused proteins) or HisTrap HP (His_6-tagged proteins) (GE Healthcare, Little Chalfont, UK). Mutant RBD proteins were generated by site-specific polymerase chain reaction (PCR) mutagenesis and confirmed by sequencing analysis. Mutant RBDs containing a C-terminal His_6 tag were transiently expressed in 293T cell supernatants and purified by HisTrap HP as described above.

2.3. Generation of humanized mAb hMS-1

The hMS-1 mAb was generated by humanizing the murine mAb Mersmab1 using a previously described protocol (Boulianne et al., 1984). Briefly, total RNA was isolated from the Mersmab1 hybridoma cells and used to synthesize cDNA. Primers mVH-f (5′ ATG GRA TGG AGC TGG ATC TT 3′) and mVH-r (5′ ATA GAC AGA TGG GGG TGT CGT TTT GGC 3′) were used to amplify the variable region of the heavy chain (V_H) gene, and mVK-f (5′ ATG GAG WCA GAC ACA CTC CT 3′) and mVK-r (5′ GGA TACA GTT GGT GCA GCA TC 3′) (Du et al., 2013a) were used for the variable region of the light chain (V_L) gene. Sequence-confirmed V_H and V_L genes were inserted into the pRBO/Ig expression vector (containing human IgG1-and human immunoglobulin kappa chain constant regions). Recombinant plasmid was transfected into 293F cells and humanized mAb was purified from the cell culture supernatants. Purified hMS-1 mAbs were resolved by reducing 12% sodium dodecyl sulphate-polyacrylamide electrophoresis (SDS-PAGE) and non-reducing 8% SDS-PAGE, respectively.

2.4. Enzyme-linked immunosorbent assay (ELISA)

The reactivity of hMS-1 and MERS-CoV RBD was detected by ELISA as described (Du et al., 2014). Briefly, ELISA plates were coated overnight at 4 °C with His_6-tagged RBD protein (1 μg/ml) and blocked with 2% no-fat milk at 37 °C for 2 h. Serial diluted hMS-1 or trastuzumab control (Roche, Roswell, GA, USA) was added to the plates and incubated at 37 °C for 1 h. Horseradish peroxidase-conjugated goat anti-human IgG (1:5,000, Santa Cruz Biotechnology, Dallas, TX, USA) was then added and further incubated at 37 °C for 1 h. The reaction was visualized by TMB substrate addition (Invitrogen, Carlsbad, CA, USA) and stopped by 1N H_2SO_4. The absorbance at 450 nm was measured using an ELISA plate reader (BioTek, Winooski, VT, USA). The half-maximal effective concentration (EC_{50}) of hMS-1 was calculated using GraphPad Prism 5.01 software (La Jolla, CA, USA). hMS-1 epitope mapping was performed by ELISA as described above except that the ELISA plates were coated with a series of mutant RBD proteins (2.5 μg/ml).

2.5. Surface plasmon resonance (SPR)

The affinity of hMS-1 binding to the MERS-CoV RBD was assayed using a Biacore T100 instrument (GE Healthcare, Little Chalfont, UK). hMS-1 (5 μg/ml) was immobilized on a CM5 sensor chip with an amine coupling kit. The reference flow cell was treated with amine coupling reagent without exposure to hMS-1. The running buffer was HBS-EP (10 mM HEPES, pH 7.4, 150 mM NaCl, 3 mM EDTA, and 0.05% surfactant P20). His_6-tagged RBD protein at gradient concentrations (2, 4, 8, 16, and 32 nM) was flowed over the chip surface. The chip was regenerated with 100 mM H_3PO_4. The sensorgram was analyzed using BIAevaluation software, and the data were fitted to a 1:1 binding model.

2.6. MERS-CoV neutralization assay

The *MERS-CoV* neutralization assay was performed as described (Du et al., 2013b; Tao et al., 2013). Briefly, serially 2-fold-diluted hMS-1 or a trastuzumab control was incubated with 100 50% tissue culture infective doses ($TCID_{50}$) of MERS-CoV at 37 °C for 1 h followed by incubation with Vero cells at 37 °C for 72 h. The cytopathic effect (CPE) was observed daily and recorded on day 3 following inoculation. The 50% neutralizing dose (ND_{50}) was calculated by the Reed-Muench method (Reed and Muench, 1938) and determined as the antibody concentration that completely inhibited virus-induced CPE in at least 50% of the wells.

2.7. Flow cytometric analysis

Determination of the hMS-1 inhibitory ability against the binding between MERS-CoV RBD and hDPP4-expressing Huh-

7 cells was performed by flow cytometry as described (Du et al., 2013b). Briefly, Huh-7 cells (5×10^5) were incubated with Fc-fused RBD protein (2 μg/ml) in the presence of serially diluted hMS-1 or with the trastuzumab control at room temperature for 30 min, followed by incubation with DyLight 488-labeled goat anti-human IgG antibody at room temperature for 30 min. The fluorescence signals were analyzed by flow cytometry (Guava, EMD Millipore, Germany).

2.8. Pseudovirus neutralization assay

The pseudovirus neutralization assay was performed as described (Zhao et al., 2013). Briefly, 293T cells were co-transfected with plasmids encoding an Env-defective, luciferase-expressing HIV-1 genome (pNL4-3.luc.RE) and encoding the MERS-CoV spike protein (EMC2012 strain) or MERS-CoV emergent strains with the corresponding RBD mutations, to package pseudotyped MERS-CoVs. Pseudoviruses were incubated with serially diluted hMS-1 at 37 °C for 1 h and the mixture was then added to Huh-7 cells pre-plated in 96-well tissue culture plates (10^4/well) 6 h before inoculation. After 72 h, the cells were lysed with cell lysis buffer (Promega, Madison, WI, USA) and transferred into 96-well luminometer plates. The luciferase activity was determined using an Infinite M1000 luminometer (Tecan, San Jose, CA, USA). ND_{50} was calculated using the dose-response inhibition model in GraphPad Prism.

2.9. Multiple sequence alignment of MERS-CoV RBDs

A total of 278 full-length spike protein sequences were collected from the MERS Coronavirus Database of The Virus Variation Resource (Brister et al., 2014) for multiple sequence alignment using the MUSCLE program (Edgar, 2004). GenBank accession numbers of selected MERS-CoV isolates are listed in Supplementary materials and methods.

2.10. Animal infection and antiviral therapy

We used 8–10-week-old female hDPP4-Tg mice to evaluate the hMS-1 passive therapeutic effect against lethal MERS-CoV infection (Zhao et al., 2015). Following intraperitoneal anesthetization with sodium pentobarbital (5 mg/kg of body weight), mice under lethal virus infection were intranasally inoculated with $10^{4.6}$ $TCID_{50}$ MERS-CoV (EMC2012 strain) in 20 μl Dulbecco's modified Eagle's medium (DMEM). After 24 h, the mice were intravenously injected with 2 mg/kg purified hMS-1 or the trastuzumab mAb control. Infected mice were observed for 23 days to calculate the body weight change and survival rate. Additionally, 5 mice were sacrificed from each group on day 3 post-infection and lung tissues were collected for virological detection and histopathological evaluation.

2.11. Viral titer detection

Viral titer was detected as described (Zhao et al., 2015). Briefly, mouse lung tissues were homogenized in DMEM plus antibiotics to achieve 10% (w/v) suspensions, which were then titrated on monolayers of Vero cells in quadruplicate. The CPE was observed daily under phase-contrast microscopy for 3 days. The viral titer was calculated by the Reed-Muench method and expressed as $\log_{10}TCID_{50}$/g of tissue.

2.12. Histopathology analysis

Collected tissues were immediately fixed in 10% neutral buffered formalin and then embedded in paraffin. Sections (4 μm in thickness) were generated, mounted onto slides, and stained by hematoxylin and eosin (H&E). Histopathological changes were observed using light microscopy. The extent of lung injury was scored according to the levels of degeneration and necrosis of the bronchi and bronchiolar epithelium, infiltration of inflammatory cells, alveoli degeneration and collapse, expansion of the parenchymal wall, hemorrhage, and interstitial edema (Sun et al., 2013).

2.13. Statistics

Statistical analyses were performed using GraphPad Prism version 5.01. The significance between survival curves was analyzed by Kaplan-Meier survival analysis with a log-rank test. Other data were analyzed using the 2-tailed unpaired *t*-test with Welch's correction. $p < 0.05$ was considered significant.

3. Results

3.1. Humanized mAb hMS-1 binds to MERS-CoV RBD with high affinity

Humanized mAb hMS-1 was expressed in 293F cells and purified by HiTrap Protein A FF. Reducing and non-reducing SDS-PAGE showed that hMS-1 migrated as a single protein of approximately 180 kDa and dissociated into heavy and light chains of about 50 and 26 kDa under reducing conditions (Fig. 1A and B), in accordance with the characteristics of a humanized antibody. The reactivity of hMS-1 to MERS-CoV RBD was subsequently measured by ELISA. As shown in Table 1, hMS-1 maintained the ability of the parental Meramb1 mAb to react strongly with MERS-CoV RBD, with an EC_{50} of 1.67 μg/ml. Comparatively, the trastuzumab control did not react with RBD (data not shown). The interaction between hMS-1 and MERS-CoV RBD was also characterized by SPR, showing a K_d of 44.7 pM. These results suggest that a humanized mAb, hMS-1, was successfully generated, which exhibited high affinity MERS-CoV RBD binding.

3.2. Humanized mAb hMS-1 neutralizes MERS-CoV infection by blocking the binding of MERS-CoV RBD to the hDPP4 receptor

The neutralizing activity of hMS-1 against live MERS-CoV infection was determined. hMS-1 could potently neutralize infection of live MERS-CoV (EMC2012 strain) in permissive Vero cells with an ND_{50} of 3.34 μg/ml (Table 1) whereas trastuzumab did not exhibit antiviral activity against MERS-CoV infection. These results suggest that humanized hMS-1 maintained the potent ability to neutralize MERS-CoV infection.

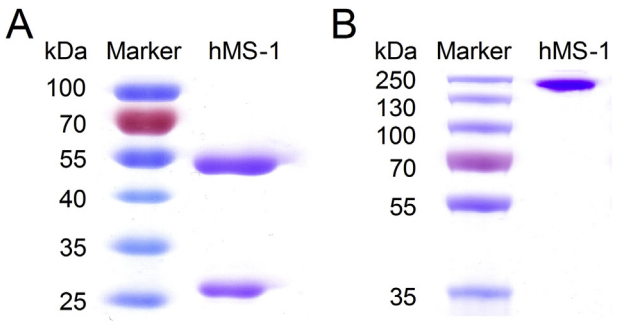

Fig. 1. Analysis of hMS-1 expression. The expression of hMS-1 was resolved by reducing 12% SDS-PAGE (A) and non-reducing 8% SDS-PAGE (B) respectively, followed by Coomassie blue staining. Prestained protein molecular-weight markers (kDa) (Thermo Scientific) are indicated on the left of each panel.

Table 1
Characteristics of humanized hMS-1 mAb.

	Binding kinetics[a]			EC_{50} (μg/ml)[b]	ND_{50} (μg/ml)[c]
	k_{on} ($M^{-1}\cdot s^{-1}$)	k_{off} (s^{-1})	K_D (M)		
hMS-1	1.82×10^6	8.17×10^{-5}	4.47×10^{-11}	1.67	3.34

[a] The binding kinetics of hMS-1 to MERS-CoV RBD was measured by BIAcore.
[b] The RBD-specific reactivity (EC_{50}) of hMS-1 was determined by ELISA.
[c] The neutralizing activity (ND_{50}) of hMS-1 was determined using a live MERS-CoV-based neutralization assay.

Since hMS-1 targeted the MERS-CoV RBD, its neutralization mechanism was thus investigated by measuring its ability to block the binding between MERS-CoV RBD and the hDPP4 receptor by flow cytometric analysis (Du et al., 2014). Whereas high fluorescence intensity was detected in Huh-7 cells incubated with RBD protein alone, only background fluorescence levels were observed in the RBD-Huh-7 binding samples in the presence of hMS-1 at 5 μg/ml. This suggested that hMS-1 was able to strongly block the binding between MERS-CoV RBD and cell-associated hDPP4 (Fig. 2A) and that the blocking effect occurred in a dose-dependent manner (Fig. 2B). In contrast, trastuzumab did not affect MERS-CoV RBD binding to the DPP4-expressing Huh-7 cells (Fig. 2A and B). These results strongly suggest that hMS-1 neutralized MERS-CoV infection by inhibiting the binding of MERS-CoV RBD to hDPP4.

3.3. Humanized mAb hMS-1 recognizes conserved RBD epitopes and cross-neutralizes MERS-CoV evolutionary strains

To identify the epitopes on the MERS-CoV RBD recognized by hMS-1, we utilized a panel of mutant RBD proteins generated by mutating the key residues at the MERS-CoV RBD and the hDPP4 binding interface to alanine (Du et al., 2014); the binding between hMS-1 and the respective mutant RBD proteins was then measured by ELISA as described (Gao et al., 2013; Lu et al., 2013). hMS-1 was not capable of recognizing the RBD of the R511A mutant and reduced its binding to RBDs with mutations at D510A and W553A, respectively (Fig. 3A). In comparison, the remaining mutations on the RBD did not affect the binding between hMS-1 and RBD with the exception of L506A, which exhibited a slight loss of binding activity. A pseudovirus neutralization assay further revealed that pseudotyped MERS-CoV expressing the spike protein containing R511A, D510A, or W553A mutants completely abolished (R511A), or reduced (D510A or W553A) the inhibitory effect of hMS-1 on pseudovirus infection. In contrast, L506A did not change the ability of hMS-1 to inhibit MERS pseudovirus infection (Fig. 3B). These results indicate that the R511 residue of RBD is a crucial neutralizing epitope recognized by hMS-1.

Alignment of 278 full-length spike protein sequences deposited in the NCBI MERS-CoV database illustrated that the RBD epitope recognized by hMS-1 is highly conserved among MERS-CoV emergent isolates (Supplementary Fig. 1). In particular, the R511 residue was not naturally mutated during MERS-CoV evolution, indicating the ability of hMS-1 to cross-neutralize MERS-CoV emergent strains. To further understand whether the natural RBD mutations of the evolved strains of MERS-CoV isolated from the 2012 to 2015 outbreaks affected the hMS-1 neutralizing activity, we constructed a series of pseudoviruses expressing MERS-CoV spike proteins with these mutated RBD residues. hMS-1 exhibited potent neutralizing activities toward all MERS mutant pseudoviruses tested, with ND_{50} values ranging from 0.009 to 0.091 μg/ml (Table 2). These results suggest that hMS-1 exhibits the ability to cross-neutralize emergent MERS-CoV isolates.

3.4. Single-dose treatment of humanized mAb hMS-1 provides full protection from lethal MERS-CoV infection in the hDPP4-Tg mouse model

Because wild-type mice are not permissive to MERS-CoV infection (Coleman et al., 2014), the passive immunotherapeutic effect of hMS-1 was evaluated in the hDPP4-Tg mouse model in

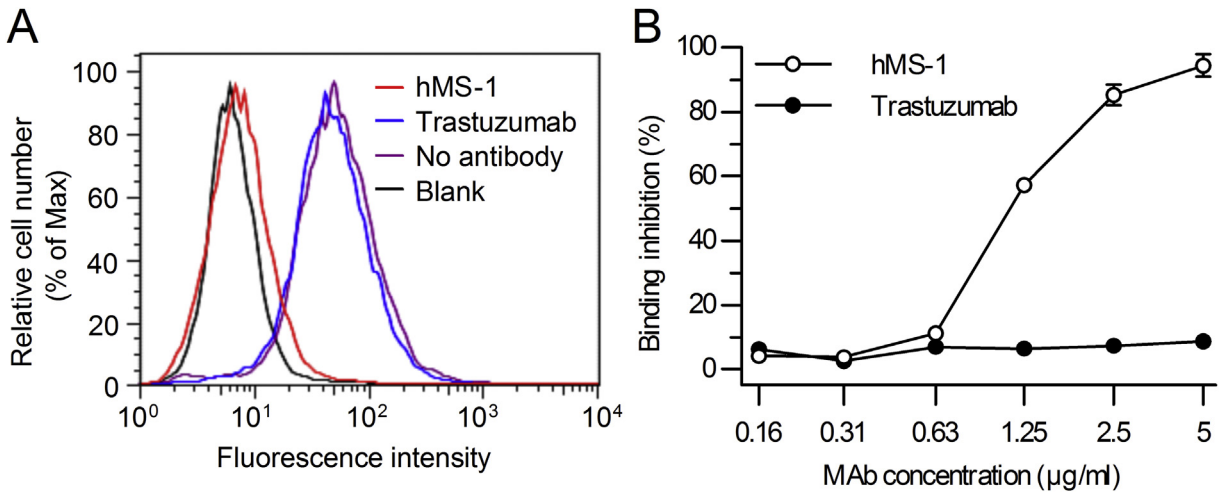

Fig. 2. hMS-1 blocks the binding between MERS-CoV RBD and the hDPP4 receptor. The blocking effect of hMS-1 on the cell-binding activity of MERS-CoV RBD was determined by flow cytometric analysis. (A) Blockage of Fc-fused MERS-CoV RBD protein binding to Huh-7 cells by 20 μg/ml hMS-1. Black line, Huh-7 cell control; purple line, binding of Fc-fused RBD to Huh-7 cells in the absence of antibody; blue line, irrelevant Trastuzumab mAb control; red line, MERS-CoV RBD binding of Huh-7 cells in the presence of hMS-1. (B) Flow cytometric analysis shows that hMS-1 inhibited the binding between the Fc-fused RBD protein and Huh-7 cells in a dose-dependent manner. The data are presented as the mean percentages of inhibition ± SEM (n = 3). (For interpretation of the references to colour in this figure legend, the reader is referred to the web version of this article.)

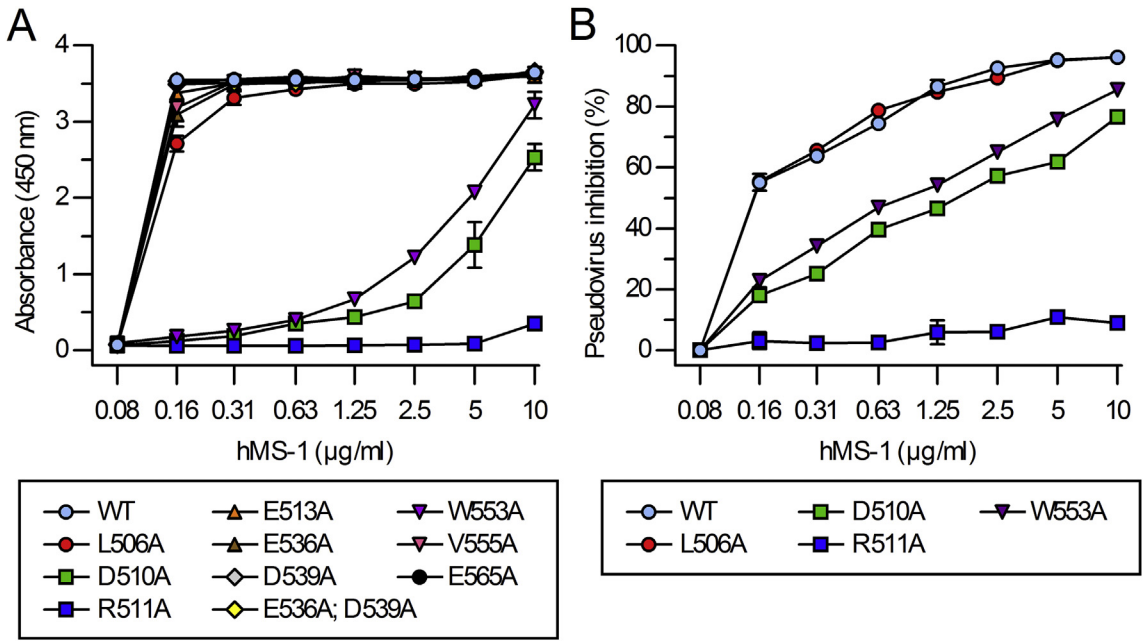

Fig. 3. Mapping of epitopes recognized by hMS-1 in MERS-CoV RBD. (A) Binding of hMS-1 to RBD mutant proteins as detected by ELISA. (B) Neutralizing activity of hMS-1 to pseudovirus mutants in a pseudovirus-based neutralization assay. Data are presented as the means ± SEM (n = 2). Protein and pseudovirus without mutations served as the wild type (WT) controls.

Table 2
Cross-neutralizing activities of hMS-1 against pseudotyped MERS-CoV mutants[a].

Accession No.	Representative isolates	Country	Isolate date	RBD mutations[b]	ND_{50} (μg/ml)
AFS88936	EMC2012	Saudi Arabia	2012/6/13	— [c]	0.089
AFY13307	England 1	United Kingdom	2012/9/11	L506F	0.049
AHI48725	Asir_1c_2013	Saudi Arabia	2013/7/2	A434V	0.044
AHI48528	Riyadh_9_2013	Saudi Arabia	2013/7/17	A431P; A482V	0.087
AHC74088	Qatar3	Qatar	2013/10/13	S460F	0.023
AID55087	Jeddah_C9313/KSA/2014	Saudi Arabia	2014	Q522H	0.044
AID55090	Riyadh_2014KSA_059/KSA/2014	Saudi Arabia	2014	T424I	0.009
AKL59401	KOR/KNIH/002_05_2015	South Korea	2015/5/20	V530L	0.091
ALJ54520	Hu/Hufuf-KSA-12597/2015	Saudi Arabia	2015/6/13	V534A	0.039

[a] A pseudovirus-based neutralization assay was performed to evaluate the cross-neutralization of hMS-1 against different MERS-CoV isolates. Pseudotyped MERS-CoV mutants were generated containing corresponding RBD mutations in the spike protein of MERS-CoV representative isolates from years 2012–2015.
[b] RBD residues mutated in the spike proteins of the respective pseudotyped MERS-CoV mutants are indicated.
[c] The pseudotyped MERS-CoV expressing the spike protein of the EMC2012 strain was considered to be the prototype pseudovirus. ND_{50} was determined by using a pseudotyped MERS-CoV-based neutralization assay.

which MERS-CoV infection can lead to a fatal outcome. After 24 h following lethal infection of MERS-CoV ($10^{4.6}$ $TCID_{50}$ EMC2012), hDPP4-Tg mice were intravenously injected with a single-dose (2 mg/kg) of hMS-1 or the trastuzumab mAb control and viral titers, histopathological changes, body weight changes, and survival rates were calculated. Viral titers were measured from mouse lungs at three days following viral infection; these demonstrated that mice receiving hMS-1 treatment exhibited significantly lower viral titers than those receiving the trastuzumab mAb control ($p < 0.01$) (Fig. 4A), suggesting that hMS-1 can inhibit MERS-CoV infection *in vivo*. Further examination of associated histopathological changes illustrated that hMS-1 treatment significantly alleviated the lung injury induced by MERS-CoV infection ($p < 0.01$) (Fig. 4B). The hMS-1-treated hDPP4-Tg mice under lethal MERS-CoV infection exhibited fewer histopathological changes (Fig. 4C–F), and were accompanied by only a small degree of inflammatory cell infiltration in the lung interstitial tissues (Fig. 4E, F). In contrast, severe lung damage was observed in the control mice (Fig. 4G–J), which developed marked interstitial pneumonia with focal exudation (Fig. 4H), macrophage infiltration (Fig. 4I), hemorrhage (Fig. 4J), and alveolar septal thickening (Fig. 4H, J). In addition, hMS-1-treated mice exhibited only slight decreases of body weight by day 11 followed by subsequent recovery, whereas control mice demonstrated dramatic body weight loss (Fig. 5A). Notably, all hMS-1-treated mice survived lethal MERS-CoV infection whereas all control group animals died by day 10 post-infection ($p < 0.01$) (Fig. 5B). These results confirmed that single-dose hMS-1 mAb treatment was able to completely protect hDPP4-Tg mice from lethal MERS-CoV infection.

4. Discussion

MERS-CoV infects humans with high associated mortality, posing a large threat to public health and reinforcing the urgency to develop effective vaccines and therapeutics. A number of therapeutic mAbs have been applied clinically to prevent and treat viral infections (Murray et al., 2014; Qiu et al., 2014), suggesting that neutralizing mAbs might represent a promising approach to combat MERS-CoV infection as well. The MERS-CoV RBD can elicit strong neutralizing antibody response and contains a critical

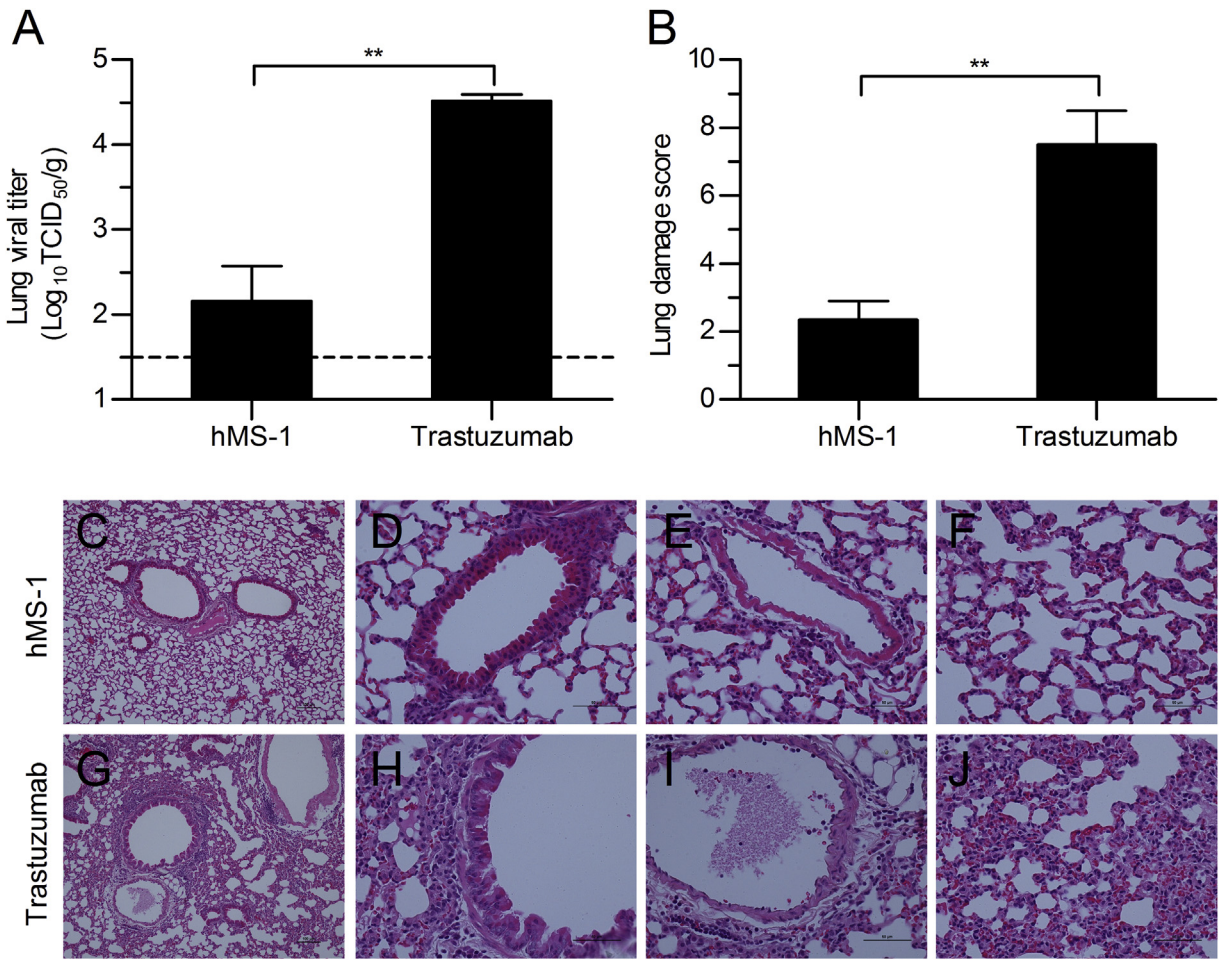

Fig. 4. Therapeutic treatment with hMS-1 limits lung viral replication and alleviates lung injury induced by MERS-CoV infection. (A) Viral titers detected in the mouse lung at day 3 post-infection (n = 5). The data are expressed as the means ± SEM. $^{**}p < 0.01$. The dotted line indicates the limit of detection. (B) Semiquantitative histopathological analysis of H&E-stained lung sections from mice sacrificed at day 3 post-infection (n = 5). The data are expressed as the means ± SEM. $^{**}p < 0.01$. (C–J) Representative H&E-stained lung sections of hMS-1- and Trastuzumab-treated hDPP4 Tg mice, including locations on the trachea (D, H), vessel (E, I), and interstitial area (F, J) (scale bars, 100 μm for C, G; 50 μm for D–F, H–J).

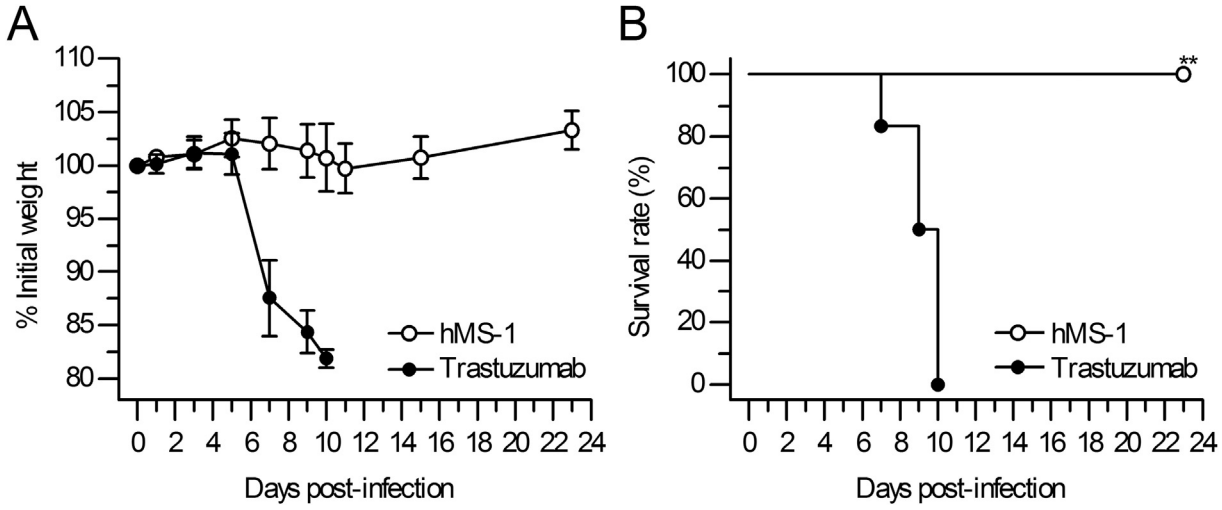

Fig. 5. Single-dose treatment of hMS-1 fully protects hDPP4 transgenic mice from lethal MERS-CoV infection. The hDPP4 transgenic mice were administered a single-dose of hMS-1 or the irrelevant Trastuzumab 24 h after lethal infection of MERS-CoV and then monitored for 23 days. (A) Body weight changes of hMS-1- and Trastuzumab-treated mice. Results are expressed as the means ± SEM (n = 6). (B) Survival rate (%) of hMS-1- and Trastuzumab-treated mice (n = 6). $^{**}p < 0.01$.

neutralizing domain (Ma et al., 2014; Zhang et al., 2016), thus representing an ideal target for neutralizing mAb development. Notably, almost all reported MERS-CoV neutralizing mAbs including murine, human, and humanized mAbs, target the RBD (Corti et al., 2015; Du et al., 2014; Jiang et al., 2014; Li et al., 2015; Pascal et al., 2015; Tang et al., 2014; Ying et al., 2014; Yu et al., 2015). We previously developed an RBD-targeting murine neutralizing mAb, Mersmab1, and demonstrated its ability to neutralize MERS-CoV infection (Du et al., 2014). Here, we further humanized this mAb and evaluated its binding affinity to RBD, inhibitory ability against RBD-hDPP4 binding, and neutralizing and cross-neutralizing activity against divergent MERS-CoV strains isolated from the 2012–2015 outbreaks. The therapeutic potential of the humanized hMS-1 mAb was also investigated in hDPP4-Tg mice.

Our data clearly showed that humanized hMS-1 mAb maintained strong reactivity to the RBD, significantly blocking RBD/hDPP4 receptor binding and potently neutralizing MERS-CoV infection. As it has been demonstrated that MERS-CoV underwent evolution during the 2012–2015 outbreaks (Cotten et al., 2013; Sabir et al., 2016), we evaluated the hMS-1 cross-neutralizing activity against these MERS-CoV emergent strains. hMS-1 recognized three key residues (neutralizing epitopes) of MERS-CoV RBD all of which were highly conserved during MERS-CoV evolution, leading to the hypothesis that hMS-1 might be effective in combatting the infections of different MERS-CoV emerging isolates. Notably, hMS-1 could potently neutralize a series of pseudoviruses expressing the spike proteins of MERS-CoVs isolated from outbreaks in different regions including Saudi Arabia and South Korea over the 2012–2015 period, demonstrating its cross-neutralizing activity against MERS-CoV spread and evolution.

Several neutralizing mAbs including LCA60, REGN3051, REGN3048, 4C2h, and m336 have been tested *in vivo* for their protective efficacy using non-lethal MERS-CoV challenge mouse or rabbit models (Corti et al., 2015; Li et al., 2015; Pascal et al., 2015; Houser et al., 2016). In this study, we evaluated the protective efficacy of hMS-1 in a lethal hDPP4-Tg mouse model, wherein we demonstrated that a single-dose (2 mg/kg) of hMS-1 completely protected hDPP4-Tg mice from a lethal challenge from MERS-CoV. This study therefore suggests that hMS-1 might be further developed as a potent passive therapeutic agent to treat patients infected with MERS-CoV.

Acknowledgements

This work was supported by the China National Program of Infectious Disease fund 2014ZX10004001004, an NIH grant (R21AI109094), and an intramural fund of the New York Blood Center (NYB000348). The authors declared no conflict of interest.

Appendix A

MERS-CoV isolates for multiple sequence alignment.

A total of 278 full-length of spike proteins of MERS-CoV isolates were collected for multiple sequence alignment. GenBank Accession numbers of collected sequences are listed as follows. AIZ74439; AHL18090; ALS20350; AGH58717; AHY21469; AKM76239; AHY22565; ALJ54461; ALR69641; AHX00711; AHX00721; AHX00731; AHY22555; ALJ54472; ALA49649; AKN24812; ALB08311; ALB08322; ALJ54451; ALJ54455; ALJ54490; ALJ54456; AJG44069; AIY60578; AJG44058; AJG44091; AKM76229; AJG44080; ALA49803; ALA49814; ALJ54474; ALA49671; AHI48528; AKL59401; AKN24803; ALA49660; ALJ54471; ALJ54517; ALJ54495; AJG44102; AJG44113; ALJ54452; ALW82753; AIZ74433; AHB33326; AIZ74417; AIZ74450; AJG44124; ALT66870; ALT66880; AIY60518; AIY60538; AIY60548; AIY60558; AIY60568; AIY60588; AIY60528; AHI48550; AGN52936; AFS88936; AGV08390; AFY13307; AGG22542; AHE78097; AHE78108; AHI48594; AHI48605; AHN10812; AHI48583; ALA49374; ALA49693; ALA49704; AHZ58501; AID55073; AKN24749; AKN24758; AKN24767; AKN24776; AKN24785; AKN24794; AKN24821; AKN24830; ALA49396; ALA49407; ALA49418; ALA49429; ALA49836; ALA49902; ALA49946; ALA50067; ALA49385; ALA49550; ALA49561; ALA49572; ALA49616; ALA49627; ALA49638; ALA49682; ALA50034; ALA50045; ALJ54475; ALJ54477; ALJ54478; ALJ54479; ALJ54480; ALJ54493; ALJ54450; ALJ54481; ALJ54484; ALJ54486; ALJ54496; ALW82691; ALJ54518; ALA49341; ALJ54446; ALJ54468; AGN70929; AGN70951; AGN70962; AGN70973; AGV08444; AGV08480; AGV08535; AGV08546; AGV08558; AGV08573; AHI48517; AGV08492; ALA49473; ALA49495; ALA49462; ALA49484; ALA49506; ALA49517; ALA49528; ALA49539; ALA49583; ALA49594; ALA49605; ALA49715; ALA49726; ALA49737; ALA49748; ALA49759; ALA49770; ALA49781; ALA49792; ALJ54502; AID55066; AID55067; AID55068; AID55069; AID55070; AID55071; AID55072; AHZ64057; AIZ48760; ALJ54501; ALD51904; AGV08467; AHX71946; AHY22545; AJD81440; ALA49363; ALA49451; ALJ54453; ALJ54467; ALJ54491; ALJ54500; ALJ54508; ALJ54512; ALJ54516; ALJ54521; ALW82742; AGV08379; AGV08408; AGV08584; ALJ54520; AHC74088; AHC74098; ALA49352; ALJ54463; ALA49957; ALA49968; ALB08246; ALB08257; ALJ54458; ALJ54483; ALJ54488; ALJ54497; AGV08455; AHI48539; AHI48561; AKI29255; AKI29265; AKI29275; AKI29284; ALJ54441; ALJ54442; ALJ54443; ALB08267; ALB08278; ALB08289; ALB08300; ALJ54448; ALJ54465; ALJ54466; AHI48572; AHY22525; AHY22535; AID50418; AJD81451; AKJ80137; AKK52582; AKK52592; AKK52602; AKK52612; AKQ21055; AKQ21064; AKQ21073; ALA49440; ALA49825; ALA49847; ALA49858; ALA49869; ALA49880; ALA49891; ALA49913; ALA49924; ALA49935; ALA49979; ALA49990; ALA50001; ALA50012; ALA50023; ALA50056; ALJ54444; ALJ54445; ALJ54447; ALJ54449; ALJ54454; ALJ54457; ALJ54459; ALJ54460; ALJ54462; ALJ54464; ALJ54469; ALJ54470; ALJ54473; ALJ54476; ALJ54482; ALJ54485; ALJ54487; ALJ54489; ALJ54492; ALJ54494; ALJ54498; ALJ54499; ALJ54503; ALJ54504; ALJ54505; ALJ54506; ALJ54507; ALJ54509; ALJ54510; ALJ54511; ALJ54513; ALJ54514; ALJ54515; ALJ54519; ALW82636; ALW82647; ALW82658; ALW82669; ALW82680; ALW82709; ALW82720; ALW82731.

Appendix. BSupplementary data

Supplementary data related to this article can be found at http://dx.doi.org/10.1016/j.antiviral.2016.06.003.

References

Bonavia, A., Zelus, B.D., Wentworth, D.E., Talbot, P.J., Holmes, K.V., 2003. Identification of a receptor-binding domain of the spike glycoprotein of human coronavirus HCoV-229E. J. Virol. 77, 2530–2538.

Boulianne, G.L., Hozumi, N., Shulman, M.J., 1984. Production of functional chimaeric mouse/human antibody. Nature 312, 643–646.

Brister, J.R., Bao, Y., Zhdanov, S.A., Ostapchuck, Y., Chetvernin, V., Kiryutin, B., Zaslavsky, L., Kimelman, M., Tatusova, T.A., 2014. Virus variation resource—recent updates and future directions. Nucleic Acids Res. 42, D660–D665.

Coleman, C.M., Matthews, K.L., Goicochea, L., Frieman, M.B., 2014. Wild-type and innate immune-deficient mice are not susceptible to the Middle East respiratory syndrome coronavirus. J. General Virol. 95, 408–412.

Corti, D., Zhao, J., Pedotti, M., Simonelli, L., Agnihothram, S., Fett, C., Fernandez-Rodriguez, B., Foglierini, M., Agatic, G., Vanzetta, F., Gopal, R., Langrish, C.J., Barrett, N.A., Sallusto, F., Baric, R.S., Varani, L., Zambon, M., Perlman, S., Lanzavecchia, A., 2015. Prophylactic and postexposure efficacy of a potent human monoclonal antibody against MERS coronavirus. Proc. Natl. Acad. Sci. U. S. A. 112, 10473–10478.

Cotten, M., Watson, S.J., Kellam, P., Al-Rabeeah, A.A., Makhdoom, H.Q., Assiri, A., Al-

Tawfiq, J.A., Alhakeem, R.F., Madani, H., AlRabiah, F.A., Hajjar, S.A., Al-nassir, W.N., Albarrak, A., Flemban, H., Balkhy, H.H., Alsubaie, S., Palser, A.L., Gall, A., Bashford-Rogers, R., Rambaut, A., Zumla, A.I., Memish, Z.A., 2013. Transmission and evolution of the Middle East respiratory syndrome coronavirus in Saudi Arabia: a descriptive genomic study. Lancet 382, 1993–2002.

de Groot, R.J., Baker, S.C., Baric, R.S., Brown, C.S., Drosten, C., Enjuanes, L., Fouchier, R.A., Galiano, M., Gorbalenya, A.E., Memish, Z.A., Perlman, S., Poon, L.L., Snijder, E.J., Stephens, G.M., Woo, P.C., Zaki, A.M., Zambon, M., Ziebuhr, J., 2013. Middle East respiratory syndrome coronavirus (MERS-CoV): announcement of the Coronavirus Study Group. J. Virol. 87, 7790–7792.

Du, L., He, Y., Zhou, Y., Liu, S., Zheng, B.-J., Jiang, S., 2009. The spike protein of SARS-CoV — a target for vaccine and therapeutic development. Nat. Rev. Microbiol. 7, 226–236.

Du, L., Jin, L., Zhao, G., Sun, S., Li, J., Yu, H., Li, Y., Zheng, B.-J., Liddington, R.C., Zhou, Y., Jiang, S., 2013a. Identification and structural characterization of a broadly neutralizing antibody targeting a novel conserved epitope on the influenza virus H5N1 hemagglutinin. J. Virol. 87, 2215–2225.

Du, L., Kou, Z., Ma, C., Tao, X., Wang, L., Zhao, G., Chen, Y., Yu, F., Tseng, C.-T.K., Zhou, Y., Jiang, S., 2013b. A truncated receptor-binding domain of MERS-CoV spike protein potently inhibits MERS-CoV infection and induces strong neutralizing antibody responses: implication for developing therapeutics and vaccines. PLoS ONE 8, e81587.

Du, L., Zhao, G., Yang, Y., Qiu, H., Wang, L., Kou, Z., Tao, X., Yu, H., Sun, S., Tseng, C.T., Jiang, S., Li, F., Zhou, Y., 2014. A conformation-dependent neutralizing monoclonal antibody specifically targeting receptor-binding domain in Middle East respiratory syndrome coronavirus spike protein. J. Virol. 88, 7045–7053.

Edgar, R.C., 2004. MUSCLE: multiple sequence alignment with high accuracy and high throughput. Nucleic Acids Res. 32, 1792–1797.

Gao, J., Lu, G., Qi, J., Li, Y., Wu, Y., Deng, Y., Geng, H., Li, H., Wang, Q., Xiao, H., Tan, W., Yan, J., Gao, G.F., 2013. Structure of the fusion core and inhibition of fusion by a heptad repeat peptide derived from the S protein of Middle East respiratory syndrome coronavirus. J. Virol. 87, 13134–13140.

Houser, K.V., Gretebeck, L., Ying, T., Wang, Y., Vogel, L., Lamirande, E.W., Bock, K.W., Moore, I.N., Dimitrov, D.S., Subbarao, K., 2016. Prophylaxis with a Middle East respiratory syndrome coronavirus (MERS-CoV)-specific human monoclonal antibody protects rabbits from MERS-CoV infection. J. Infect. Dis. 213, 1557–1561.

Jiang, L., Wang, N., Zuo, T., Shi, X., Poon, K.M., Wu, Y., Gao, F., Li, D., Wang, R., Guo, J., Fu, L., Yuen, K.Y., Zheng, B.J., Wang, X., Zhang, L., 2014. Potent neutralization of MERS-CoV by human neutralizing monoclonal antibodies to the viral spike glycoprotein. Sci. Transl. Med. 6, 234ra259.

Li, Y., Wan, Y., Liu, P., Zhao, J., Lu, G., Qi, J., Wang, Q., Lu, X., Wu, Y., Liu, W., Zhang, B., Yuen, K.Y., Perlman, S., Gao, G.F., Yan, J., 2015. A humanized neutralizing antibody against MERS-CoV targeting the receptor-binding domain of the spike protein. Cell Res. 25, 1237–1249.

Lu, G., Hu, Y., Wang, Q., Qi, J., Gao, F., Li, Y., Zhang, Y., Zhang, W., Yuan, Y., Bao, J., Zhang, B., Shi, Y., Yan, J., Gao, G.F., 2013. Molecular basis of binding between novel human coronavirus MERS-CoV and its receptor CD26. Nature 500, 227–231.

Ma, C., Wang, L., Tao, X., Zhang, N., Yang, Y., Tseng, C.T., Li, F., Zhou, Y., Jiang, S., Du, L., 2014. Searching for an ideal vaccine candidate among different MERS coronavirus receptor-binding fragments–the importance of immunofocusing in subunit vaccine design. Vaccine 32, 6170–6176.

Murray, J., Saxena, S., Sharland, M., 2014. Preventing severe respiratory syncytial virus disease: passive, active immunisation and new antivirals. Archives Dis. Child. 99, 469–473.

Pascal, K.E., Coleman, C.M., Mujica, A.O., Kamat, V., Badithe, A., Fairhurst, J., Hunt, C., Strein, J., Berrebi, A., Sisk, J.M., Matthews, K.L., Babb, R., Chen, G., Lai, K.-M.V., Huang, T.T., Olson, W., Yancopoulos, G.D., Stahl, N., Frieman, M.B., Kyratsous, C.A., 2015. Pre- and postexposure efficacy of fully human antibodies against Spike protein in a novel humanized mouse model of MERS-CoV infection. Proc. Natl. Acad. Sci. U. S. A. 112, 8738–8743.

Qiu, X., Wong, G., Audet, J., Bello, A., Fernando, L., Alimonti, J.B., Fausther-Bovendo, H., Wei, H., Aviles, J., Hiatt, E., Johnson, A., Morton, J., Swope, K., Bohorov, O., Bohorova, N., Goodman, C., Kim, D., Pauly, M.H., Velasco, J., Pettitt, J., Olinger, G.G., Whaley, K., Xu, B., Strong, J.E., Zeitlin, L., Kobinger, G.P., 2014. Reversion of advanced Ebola virus disease in nonhuman primates with ZMapp(™). Nature 514, 47–53.

Raj, V.S., Mou, H., Smits, S.L., Dekkers, D.H., Muller, M.A., Dijkman, R., Muth, D., Demmers, J.A., Zaki, A., Fouchier, R.A., Thiel, V., Drosten, C., Rottier, P.J., Osterhaus, A.D., Bosch, B.J., Haagmans, B.L., 2013. Dipeptidyl peptidase 4 is a functional receptor for the emerging human coronavirus-EMC. Nature 495, 251–254.

Reed, L., Muench, H., 1938. A simple method of estimating fifty per cent endpoints. Am. J. Hyg. 493–497.

Sabir, J.S.M., Lam, T.T.Y., Ahmed, M.M.M., Li, L., Shen, Y.E.M., Abo-Aba, S., Qureshi, M.I., Abu-Zeid, M., Zhang, Y., Khiyami, M.A., Alharbi, N.S., Hajrah, N.H., Sabir, M.J., Mutwakil, M.H.Z., Kabli, S.A., Alsulaimany, F.A.S., Obaid, A.Y., Zhou, B., Smith, D.K., Holmes, E.C., Zhu, H., Guan, Y., 2016. Co-circulation of three camel coronavirus species and recombination of MERS-CoVs in Saudi Arabia. Science 351, 81–84.

Skowronski, D.M., Astell, C., Brunham, R.C., Low, D.E., Petric, M., Roper, R.L., Talbot, P.J., Tam, T., Babiuk, L., 2004. Severe acute respiratory syndrome (SARS): a year in review. Annu. Rev. Med. 56, 357–381.

Sun, S., Zhao, G., Liu, C., Wu, X., Guo, Y., Yu, H., Song, H., Du, L., Jiang, S., Guo, R., Tomlinson, S., Zhou, Y., 2013. Inhibition of complement activation alleviates acute lung injury induced by highly pathogenic avian influenza H5N1 virus infection. Am. J. Respir. Cell Mol. Biol. 49, 221–230.

Tang, X.C., Agnihothram, S.S., Jiao, Y., Stanhope, J., Graham, R.L., Peterson, E.C., Avnir, Y., Tallarico, A.S., Sheehan, J., Zhu, Q., Baric, R.S., Marasco, W.A., 2014. Identification of human neutralizing antibodies against MERS-CoV and their role in virus adaptive evolution. Proc. Natl. Acad. Sci. U. S. A. 111, E2018–E2026.

Tao, X., Hill, T.E., Morimoto, C., Peters, C.J., Ksiazek, T.G., Tseng, C.-T.K., 2013. Bilateral entry and release of Middle East respiratory syndrome coronavirus induces profound apoptosis of human bronchial epithelial cells. J. Virol. 87, 9953–9958.

Wang, N., Shi, X., Jiang, L., Zhang, S., Wang, D., Tong, P., Guo, D., Fu, L., Cui, Y., Liu, X., Arledge, K.C., Chen, Y.H., Zhang, L., Wang, X., 2013. Structure of MERS-CoV spike receptor-binding domain complexed with human receptor DPP4. Cell Res. 23, 986–993.

Xu, Y., Lou, Z., Liu, Y., Pang, H., Tien, P., Gao, G.F., Rao, Z., 2004. Crystal structure of severe Acute respiratory syndrome coronavirus spike protein fusion core. J. Biol. Chem. 279, 49414–49419.

Ying, T., Du, L., Ju, T.W., Prabakaran, P., Lau, C.C., Lu, L., Liu, Q., Wang, L., Feng, Y., Wang, Y., Zheng, B.J., Yuen, K.Y., Jiang, S., Dimitrov, D.S., 2014. Exceptionally potent neutralization of Middle East respiratory syndrome coronavirus by human monoclonal antibodies. J. Virol. 88, 7796–7805.

Yu, X., Zhang, S., Jiang, L., Cui, Y., Li, D., Wang, D., Wang, N., Fu, L., Shi, X., Li, Z., Zhang, L., Wang, X., 2015. Structural basis for the neutralization of MERS-CoV by a human monoclonal antibody MERS-27. Sci. Rep. 5, 13133.

Zaki, A.M., van Boheemen, S., Bestebroer, T.M., Osterhaus, A.D., Fouchier, R.A., 2012. Isolation of a novel coronavirus from a man with pneumonia in Saudi Arabia. N. Engl. J. Med. 367, 1814–1820.

Zhang, N., Channappanavar, R., Ma, C., Wang, L., Tang, J., Garron, T., Tao, X., Tasneem, S., Lu, L., Tseng, C.T., Zhou, Y., Perlman, S., Jiang, S., Du, L., 2016. Identification of an ideal adjuvant for receptor-binding domain-based subunit vaccines against Middle East respiratory syndrome coronavirus. Cell Mol. Immunol. 13, 180–190.

Zhao, G., Du, L., Ma, C., Li, Y., Li, L., Poon, V.K.M., Wang, L., Yu, F., Zheng, B.-J., Jiang, S., Zhou, Y., 2013. A safe and convenient pseudovirus-based inhibition assay to detect neutralizing antibodies and screen for viral entry inhibitors against the novel human coronavirus MERS-CoV. Virol. J. 10, 266.

Zhao, G., Jiang, Y., Qiu, H., Gao, T., Zeng, Y., Guo, Y., Yu, H., Li, J., Kou, Z., Du, L., Tan, W., Jiang, S., Sun, S., Zhou, Y., 2015. Multi-organ damage in human dipeptidyl peptidase 4 transgenic mice infected with Middle East respiratory syndrome-coronavirus. PLoS One 10, e0145561.

Zhong, N.S., Zheng, B.J., Li, Y.M., Poon, L.L.M., Xie, Z.H., Chan, K.H., Li, P.H., Tan, S.Y., Chang, Q., Xie, J.P., Liu, X.Q., Xu, J., Li, D.X., Yuen, K.Y., Peiris, J.S.M., Guan, Y., 2003. Epidemiology and cause of severe acute respiratory syndrome (SARS) in Guangdong, People's Republic of China, in February, 2003. Lancet 362, 1353–1358.

Zhu, X., Guo, Y.-H., Jiang, T., Wang, Y.-D., Chan, K.-H., Li, X.-F., Yu, W., McBride, R., Paulson, J.C., Yuen, K.-Y., Qin, C.-F., Che, X.-Y., Wilson, I.A., 2013. A unique and conserved neutralization epitope in H5N1 influenza viruses identified by an antibody against the A/Goose/Guangdong/1/96 hemagglutinin. J. Virol. 87, 12619–12635.